New Carbide Clusters in the Cobalt Subgroup. Part 17.[1] Preparation and Structural Characterization of the Mixed-metal Octahedral Dianion $[Co_2Rh_4C(CO)_{13}]^{2-}$ as its $[PPh_4]^+$ Salt†

Vincenzo G. Albano,* Dario Braga, and Fabrizia Grepioni
Dipartimento di Chimica 'G. Ciamician', Universita' di Bologna, via F. Selmi 2, I-40126 Bologna, Italy
Roberto Della Pergola* and Luigi Garlaschelli
Dipartimento di Chimica Inorganica e Metallorganica, Universita' di Milano, via G. Venezian 21, I-20133 Milano, Italy
Alessandro Fumagalli
Centro di Studio per la Sintesi e la Struttura dei Composti dei Metalli di Transizione nei Bassi Stati di Ossidazione, via G. Venezian 21, I-20133 Milano, Italy

The title complex has been prepared by direct reaction of $[Co_3C(CO)_9Cl]$ with $[PPh_4][Rh(CO)_4]$ in the molar ratio 1:4 in tetrahydrofuran solution, and characterized by chemical and crystallographic methods. The anion belongs to the family of octahedral carbido-carbonyl clusters (86 valence electrons) with 13 ligands. The Co atoms are found to be contiguous with no trace of Co/Rh disorder. The ligand distribution differs from that of the analogous homometallic species $[Co_6C(CO)_{13}]^{2-}$ and $[Rh_6C(CO)_{13}]^{2-}$. The factors controlling the ligand arrangements in the three species are discussed. The compound $[PPh_4]_2[Co_2Rh_4C(CO)_{13}]$ crystallizes in the triclinic space group $P\bar{1}$, with $a = 13.358(3)$, $b = 21.981(2)$, $c = 11.526(1)$ Å, $\alpha = 94.779(9)$, $\beta = 107.62(1)$, $\gamma = 78.35(1)°$, and $Z = 2$. 6 273 Reflections were used to solve and refine the structure to $R = 0.048$, $R' = 0.058$.

We previously reported that pyrolysis of the trigonal prismatic species $[M_6C(CO)_{15}]^{2-}$ (M = Co or Rh) yields octahedral $[M_6C(CO)_{13}]^{2-}$.[1,2] The two octahedral dianions were found to be isoelectronic (86 valence electrons) but not isostructural, differing in the CO ligand distributions over the metal atom polyhedra. The factors controlling the different structural choices were unclear, although n.m.r. evidence in solution[3] suggested that interconversion of the two structures might be related to CO scrambling around the octahedral equatorial planes. In order to gain more insight into this structural problem the preparation of a mixed Co–Rh species was attempted. We now report the synthesis, chemical and structural characterization of the dianion $[Co_2Rh_4C(CO)_{13}]^{2-}$ (**1**), which not only represents the first example of an octahedral mixed-metal carbido-carbonyl cluster of Co and Rh, but also possesses an overall geometry sharing features of both $[Rh_6C(CO)_{13}]^{2-}$ (**2**)[2] and $[Co_6C(CO)_{13}]^{2-}$ (**3**),[1] thus allowing a rationalization of the steric and electronic factors controlling the ligand arrangements adopted in the three cases.

Results and Discussion

Synthesis and Chemical Characterization of $[Co_2Rh_4C(CO)_{13}]^{2-}$ (**1**).—The dianion $[Co_2Rh_4C(CO)_{13}]^{2-}$ has been obtained by treating $[Co_3C(CO)_9Cl]$ with $[PPh_4][Rh(CO)_4]$, in a 1:4 molar ratio, in tetrahydrofuran (thf) solution at room temperature. The multi-step reaction is quite slow and is completed in about 72 h, probably according to equation (1).

$$[Co_3C(CO)_9Cl] + 4\,[Rh(CO)_4]^- \longrightarrow [Co_2Rh_4C(CO)_{13}]^{2-} + Cl^- + [Co(CO)_4]^- + 8CO \quad (1)$$

Its course is not easy to follow, owing to the coincidence of the i.r. absorption bands of the anions $[Co(CO)_4]^-$ and $[Rh(CO)_4]^-$. However, when equilibrium is reached the i.r. spectrum of the red-brown solution in the carbonyl stretching region shows that all the $[Co_3C(CO)_9Cl]$ has reacted and essentially (**1**) and $[Co(CO)_4]^-$ are present. The formation of $[Co_2Rh_4C(CO)_{13}]^{2-}$ is so favoured that it is obtained even from $[Co_3C(CO)_9Cl]$ and $[Rh(CO)_4]^-$ in a 1:3 molar ratio, with some $[Co_3C(CO)_9Cl]$ left unreacted. The product can easily be separated from the by-products and recovered by fractional crystallization, yielding red-brown crystals. The i.r. spectrum (Figure 1) of $[PPh_4]_2[Co_2Rh_4C(CO)_{13}]$ in thf solution shows absorptions at 2 019vw, 1 970vs, 1 835(sh), and 1 820m cm^{-1} attributable to the terminal and edge bridging CO groups, respectively, as expected from the solid-state structure. There are no appreciable differences from the spectra of $[NEt_4]_2[Co_6C(CO)_{13}]$ and of $[PPh_4]_2[Rh_6C(CO)_{13}]$.[1,2] The anion $[Co_2Rh_4C(CO)_{13}]^{2-}$, when exposed to CO at the pressure of 1 atm (*ca.* 10^5 Pa), gives an unstable unidentified species which eventually breaks apart. This is not unexpected for a cobalt-containing cluster.[4] The most striking feature of the latter reaction is the formation of the homometallic prismatic $[Rh_6C(CO)_{15}]^{2-}$ very likely through a reconstruction process around an exposed carbide atom.

Structural Characterization.—The crystal consists of distinct $[Co_2Rh_4C(CO)_{13}]^{2-}$ anions and $[PPh_4]^+$ cations. The anion possesses an octahedral framework of metal atoms as expected for cluster species characterized by 86 valence electrons. The mixed-metal cage does not show Co–Rh disorder, and the two Co atoms occupy contiguous positions. The resulting metal atom polyhedron, incapsulating the carbide atom, is severely distorted with metal–metal bond distances in the range 2.616—3.139(1) Å. The geometry of $[Co_2Rh_4C(CO)_{13}]^{2-}$ is illustrated in Figure 2. Relevant bond distances and angles are reported in Table 1. Five ligands are found in edge-bridging positions and the remaining eight are terminally bonded. All the metal atoms are three-connected to the ligands although the Rh atoms

† Bis(tetraphenylphosphonium) μ_6-carbido-1,3;2,5;3,6;4,5;4,6-penta-μ-carbonyl-1,1,2,2,3,4,5,6-octacarbonyl-*octahedro*-1,2-dicobalt-tetrarhodate.

Supplementary data available: see Instructions for Authors, *J. Chem. Soc., Dalton Trans.*, 1989, issue 1, pp. xvii—xx.

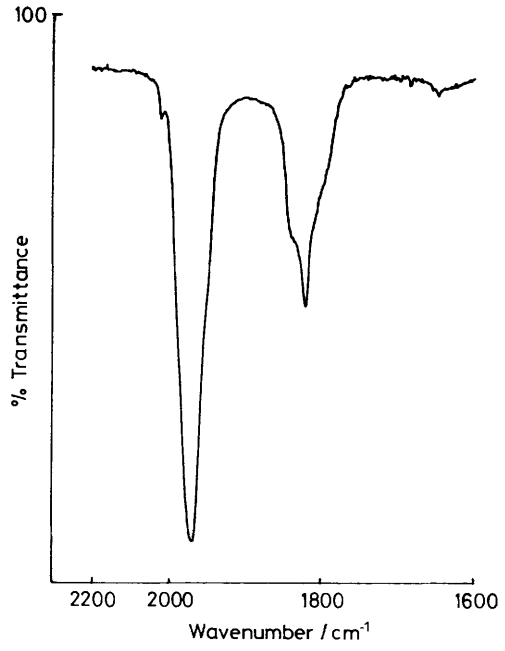

Figure 1. The i.r. spectrum of $[PPh_4]_2[Co_2Rh_4C(CO)_{13}]$ in thf solution

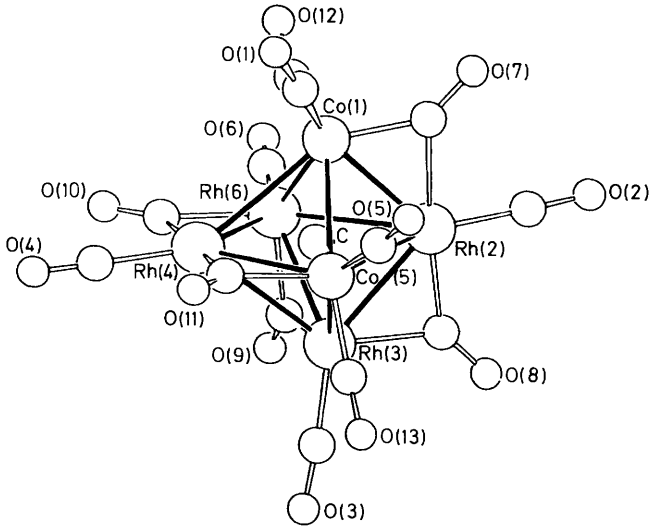

Figure 2. The structure of the dianion $[Co_2Rh_4C(CO)_{13}]^{2-}$. Carbon atoms of the CO groups bear the same numbering as the O atoms. The idealised two-fold axis passes through C(9)–O(9) and the midpoint of the Co(1)–Co(5) bond

support two bridging and one terminal ligand, while the Co atoms bear one bridging and two terminal ligands. The idealized symmetry is C_2. This ligand distribution is topologically even but electronically uneven because the cobalt atoms formally receive more electrons than the rhodium atoms.

Compound (**1**), together with the related homometallic carbides $[Rh_6C(CO)_{13}]^{2-}$ (**2**),[2] $[Co_6C(CO)_{13}]^{2-}$ (**3**),[1] and the nitride $[Co_6N(CO)_{13}]^{-}$ (**4**),[5] constitute the only examples of octahedral clusters with 13 CO ligands. Remarkably all these species, though containing the same number of ligands, adopt different ligand arrangements in the crystalline state. The distribution of the bridging ligands in (**1**)—(**3**) is sketched in Figure 3. The ligand geometry in (**1**) appears to be almost 'halfway' between those observed for the homometallic species (**2**) and (**3**). The equatorial planes with greater rhodium content

Table 1. Selected bond distances (Å) and angles (°) for compound (**1**)

Co(1)–Co(5)	2.784(2)	Rh(2)–C(8)	2.01(1)
Co(1)–Rh(2)	2.616(1)	Rh(3)–C(8)	2.06(1)
Co(1)–Rh(4)	2.955(2)	Rh(3)–C(9)	2.09(1)
Co(1)–Rh(6)	2.781(1)	Rh(6)–C(9)	2.01(1)
Co(5)–Rh(2)	3.005(1)	Rh(4)–C(10)	2.03(1)
Co(5)–Rh(3)	2.802(1)	Rh(6)–C(10)	2.01(1)
Co(5)–Rh(4)	2.680(1)	Rh(4)–C(11)	2.07(1)
Rh(2)–Rh(3)	2.765(1)	Co(5)–C(11)	1.96(1)
Rh(2)–Rh(6)	3.096(1)	Co(1)–C(12)	1.81(1)
Rh(3)–Rh(4)	3.139(1)	Rh(6)···C(12)	2.62(2)
Rh(3)–Rh(6)	2.788(1)	Rh(3)···C(13)	2.56(1)
Co(1)–C	1.903(7)	Co(5)–C(13)	1.85(2)
Co(5)–C	1.920(7)	C(1)–O(1)	1.18(2)
Rh(2)–C	2.102(8)	C(2)–O(2)	1.14(2)
Rh(3)–C	1.991(6)	C(3)–O(3)	1.18(1)
Rh(4)–C	2.123(8)	C(4)–O(4)	1.12(2)
Rh(6)–C	2.020(7)	C(5)–O(5)	1.13(3)
Co(1)–C(1)	1.74(1)	C(6)–O(6)	1.16(1)
Rh(2)–C(2)	1.87(1)	C(7)–O(7)	1.19(2)
Rh(3)–C(3)	1.86(1)	C(8)–O(8)	1.18(1)
Rh(4)–C(4)	1.88(1)	C(9)–O(9)	1.18(1)
Co(5)–C(5)	1.75(2)	C(10)–O(10)	1.20(1)
Rh(6)–C(6)	1.85(1)	C(11)–O(11)	1.17(1)
Co(1)–C(7)	1.87(1)	C(12)–O(12)	1.15(2)
Rh(2)–C(7)	2.10(1)	C(13)–O(13)	1.12(2)
Co(1)–C(1)–O(1)	172(2)	Rh(3)–C(8)–O(8)	133(1)
Rh(2)–C(2)–O(2)	178(1)	Rh(3)–C(9)–O(9)	134(1)
Rh(3)–C(3)–O(3)	175(1)	Rh(6)–C(9)–O(9)	140(1)
Rh(4)–C(4)–O(4)	180(1)	Rh(4)–C(10)–O(10)	141(1)
Co(5)–C(5)–O(5)	174(2)	Rh(6)–C(10)–O(10)	133(1)
Rh(6)–C(6)–O(6)	178(1)	Rh(4)–C(11)–O(11)	139(1)
Co(1)–C(7)–O(7)	141(1)	Co(5)–C(11)–O(11)	138(1)
Rh(2)–C(7)–O(7)	137(1)	Co(1)–C(12)–O(12)	158(1)
Rh(2)–C(8)–O(8)	142(1)	Co(5)–C(13)–O(13)	158(1)

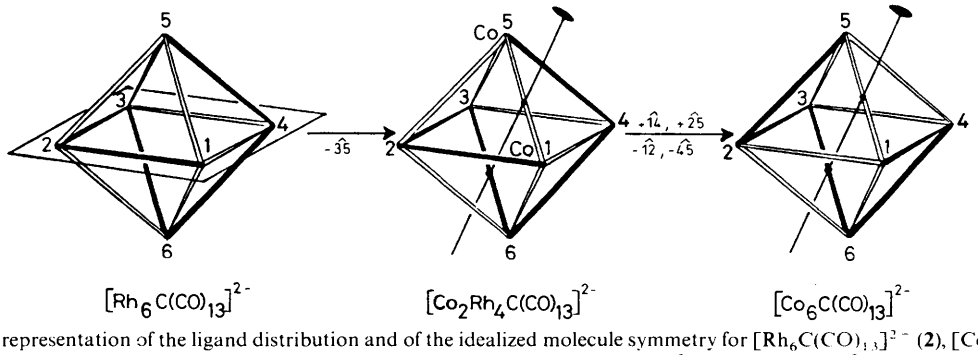

Figure 3. Schematic representation of the ligand distribution and of the idealized molecule symmetry for $[Rh_6C(CO)_{13}]^{2-}$ (**2**), $[Co_2Rh_4C(CO)_{13}]^{2-}$ (**1**), and $[Co_6C(CO)_{13}]^{2-}$ (**3**). Bridged M–M bonds are represented by solid lines, addition ($+\widehat{MM}$) or removal ($-\widehat{MM}$) of CO_b required to pass from (**1**) to (**2**), and from (**2**) to (**3**) are indicated

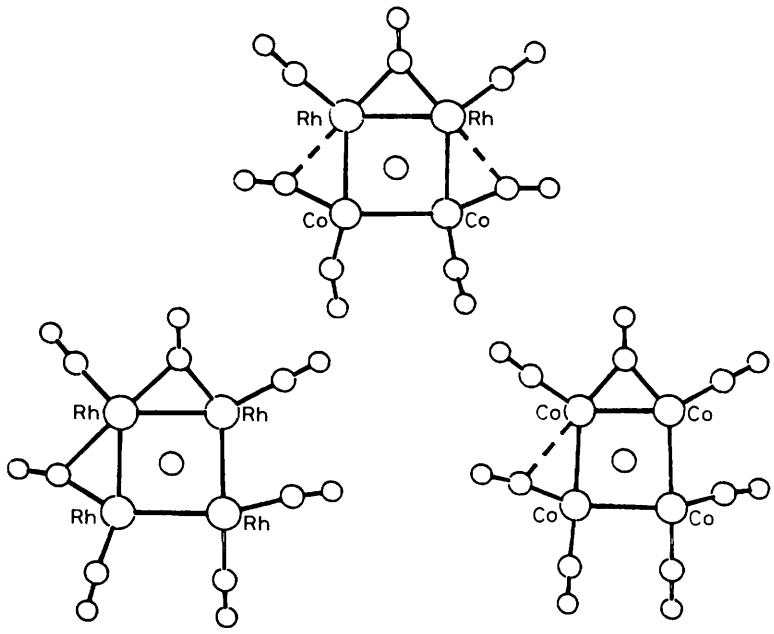

Figure 4. Comparison of the seven-CO octahedral equators of $[Rh_6C(CO)_{13}]^{2-}$, $[Co_2Rh_4C(CO)_{13}]^{2-}$, and $[Co_6C(CO)_{13}]^{2-}$, showing the smooth distribution of bridging, asymmetric bridging, and bent-terminal ligands

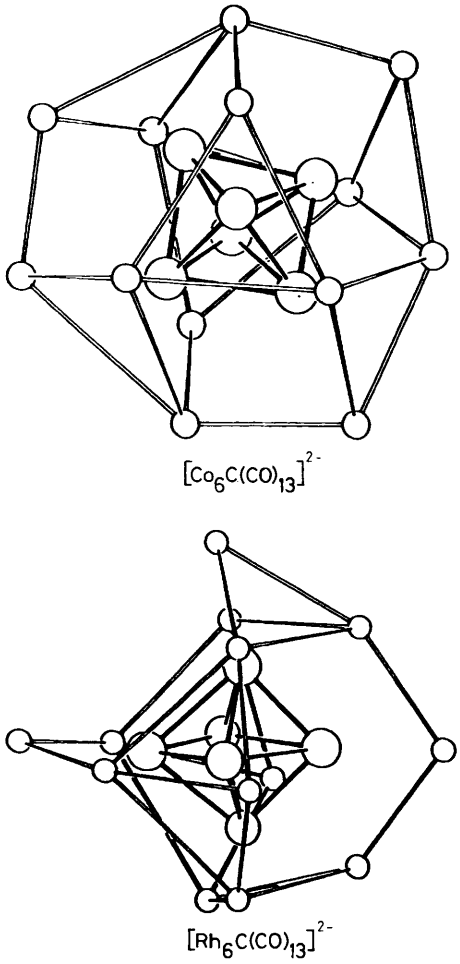

Figure 5. The outer ligand polyhedra described by the O atoms in $[Co_6C(CO)_{13}]^{2-}$ and $[Rh_6C(CO)_{13}]^{2-}$ [the ligand polyhedron of (**1**), being very similar to that of (**2**), is not reported]

[Co(1)–Rh(2)–Rh(3)–Rh(4) and Co(5)–Rh(4)–Rh(6)–Rh(2), see Figures 2 and 3] are similar to the corresponding planes in the Rh_6 cluster, while the equatorial plane with greater cobalt content [Co(1)–Rh(6)–Rh(3)–Co(5)] is more similar to the one in the Co_6 cluster. On these premises it appears that there is nothing 'fortuitous' in the adoption of different ligand distributions in the three cases, as might be assumed on the basis of the concept of 'instant stop images' relating the geometries observed in the solid state to the extensive ligand fluxionality observed in solution.[3,6] In order to get some insight into the factors governing the structures of compounds (**1**)—(**3**), further comments are necessary with reference to Figure 3. The ligand arrangement in (**2**) is converted into that in (**1**) simply by changing one ligand from bridging to terminal geometry. This results in a ligand–metal three-connection for all the atoms, a feature lacking in (**2**). The ligand distribution in (**1**), on the other hand, is changed into that of (**3**) by swapping two bridged and unbridged Rh–Co edges, with no effect on the overall symmetry and metal–ligand connectivity.

Beside the problem related to the different ligand distribution, the structure of (**1**) also offers a unique opportunity of comparing homometallic Rh–Rh and Co–Co bonding interactions and heterometallic Rh–Co interactions, both within the same system and between different, though strictly related, molecules. Comparison of metal–metal bond lengths in the two equators containing one Co atom with the values found in compound (**2**) shows that while the Rh–Co bonds are expectedly shorter than the corresponding Rh–Rh ones in $[Rh_6C(CO)_{13}]^{2-}$, the Rh–Rh distances show a slight increase which compensates for the shortening due to the substitution of Co for Rh. For instance, unbridged M–M bonds, in the two equatorial planes under examination, average 3.117(1) Å for M = M′ = Rh, and 2.980(1) Å for M = Rh, M′ = Co, while corresponding values in (**2**) are 3.080(2) and 3.130(2) Å. The same is true for M–M′ bonds spanned by CO ligands [Rh–Rh 2.761(1), Rh–Co 2.648(1) Å in (**1**); Rh–Rh 2.740(2), Rh–Rh 2.762(2) Å in (2)].

A comparison of the equatorial planes containing seven CO groups in compounds (**1**)—(**3**) is shown in Figure 4. It can be immediately noticed, on going from $[Rh_6C(CO)_{13}]^{2-}$ to $[Co_6C(CO)_{13}]^{2-}$ *via* $[Co_2Rh_4C(CO)_{13}]^{2-}$, an almost contin-

Table 2. Crystal data and details of measurements for compound (**1**)

Formula	$C_{62}H_{40}Co_2O_{13}P_2Rh_4$
M	1 584.4
Crystal size/mm	0.1 × 0.15 × 0.1
System	Triclinic
Space group	$P\bar{1}$
a/Å	13.358(3)
b/Å	21.981(2)
c/Å	11.526(1)
α/°	94.779(9)
β/°	107.62(1)
γ/°	78.35(1)
U/Å^3	3 158.2
Z	2
$F(000)$	1 560
D_c/g cm^{-3}	1.67
μ(Mo − K_α)/cm^{-1}	15.15
Scan mode	ω—2θ
θ range/°	2—25
ω scan width/°	0.8
Requested counting $\sigma(I)/I$	0.02
Pre-scan rate/min^{-1}	5
Pre-scan acceptance, $\sigma(I)/I$	0.5
Maximum scan time/s	120
Octants explored in reciprocal space	$\pm h$, $\pm k$, $+l$
Measured reflections	10 952
Unique observed reflections used in the refinement [$I_o > 2\sigma(I_o)$]	6 273
R, R'*	0.048, 0.058
k, g	0.17, 0.022

* $R' = \Sigma[(F_o - F_c)w^{\frac{1}{2}}]/\Sigma(F_o w^{\frac{1}{2}})$, where $w = k/[\sigma^2(F) + |g|F^2]$.

uous distribution of metal–ligand interactions from symmetric bridging ligands, *via* an increasing degree of asymmetry, to terminal ligands. Roughly, the bridging 'extent' (number of CO_b and degree of asymmetry) decreases on replacing Co by Rh atoms. It should also be pointed out that the shortening of the metal–metal interactions on replacing Co by Rh in these equators causes out-of-plane 'scissoring' of the terminal ligands opposite to the single CO_b in (**1**) and (**3**), clearly in order to reduce C ··· C and O ··· O repulsions.

With the knowledge of the ligand distribution in compound (**1**), is it possible to rationalize the factors determining the structural choices adopted by the two homometallic species (**2**) and (**3**). A comparison of the polyhedra described by the O atoms in (**2**) and (**3**) is shown in Figure 5. The ligand polyhedron of (**3**) can be described as a pseudo-cubo-octahedron whose equatorial vertices form a heptagon rather than a hexagon, Although this is not one of the close-packed structures predicted on the basis of a hard-sphere model for 13 CO ligands (an edge-bridged or face-capped cubo-octahedron),[7] it certainly represents a compact way of distributing these ligands on the cluster surface. The ligand distribution in compound (**2**), as well as in (**1**), determines a completely different ligand polyhedron (see Figure 5). The coverage is no longer compact, leaving large 'holes' in the ligand packing, which can be described as built up of an almost heptagonal equatorial plane plus two staggered 'fly-over' systems made up of three consecutive ligands in the other two equatorial planes.

It is worth noting that ligand–ligand interactions along the 'fly-overs' are shorter than around the equatorial plane [average O ··· O interactions 3.85 and 3.96 Å, respectively]. Moreover these interactions are also shorter than in compound (**3**) [average O ··· O contacts 4.03 Å for next-neighbouring atoms in the pseudo-cubo-octahedron]. This observation may be the key to the problem. As mentioned before, the ligand distribution in (**2**) [and in (**1**)] achieves a better charge equalization on each metal atom, while steric regularity is better attained with the pseudo-cubo-octahedral distribution present in (**3**). On these bases it appears that, when the larger Co_2Rh_4 or Rh_6 polyhedron is replaced by a smaller Co_6 one, the ligand–ligand interactions within the 'fly-over' systems might become too short and untenable (computed O ··· O interactions for an average 8% shortening of the M–M bonds are 3.57 Å), rendering the 'fly-over' arrangement no longer favoured, so that the ligand distribution 'switches' to the observed pseudo-cubo-octahedron in order to minimize ligand–ligand repulsions. In other words it appears that, on decreasing the size of the inner metal polyhedron ($Rh_6 \longrightarrow Co_2Rh_4 \longrightarrow Co_6$), the subtle balance between steric and electronic factors is altered and electronic homogeneity happens to be sacrificed first when ligand–ligand interactions become dominant. These considerations are somewhat substantiated by the fact that $[Co_6N(CO)_{13}]^-$,[5] which contains the smallest metal framework in this family of compounds {average Co–Co 2.639(1) and 2.613(5) Å in (**3**) and in $[Co_6N(CO)_{13}]^-$, respectively}, shows an outer ligand polyhedron with a further decrease in the number of CO_b (four instead of five).

Experimental

All reactions were carried out in an atmosphere of nitrogen or carbon monoxide with Schlenk-tube and vacuum-line techniques.[8] Solvents were purified and dried by distillation under a nitrogen atmosphere from the following solvent–drier combinations: thf–sodium diphenylketyl; CH_2Cl_2–P_2O_5; and cyclohexane–sodium. Infrared spectra were recorded on a Perkin-Elmer 781 spectrophotometer using calcium fluoride cells previously purged with nitrogen; the spectra were calibrated with polystyrene. The compounds $[PPh_4][Rh(CO)_4]$[9] and $[Co_3C(CO)_9Cl]$[10] were prepared as described.

Preparation of $[PPh_4]_2[Co_2Rh_4C(CO)_{13}]$.—In a Schlenk tube, under nitrogen, were placed $[PPh_4][Rh(CO)_4]$ (0.733 g, 1.33 mmol), $[Co_3C(CO)_9Cl]$ (0.168, 0.35 mmol), and thf (20 cm^3). As soon as the solvent is added the solution assumes a deep green colour, which slowly turns brown in about 3 h. After 72 h of stirring at room temperature, the solvent was removed *in vacuo* and the brown residue suspended in MeOH (25 cm^3). The suspension was allowed to stir for 3 h, then the precipitate was collected by filtration, washed with MeOH (2 × 5 cm^3), and dried. The residue was extracted from the frit with CH_2Cl_2 (15 cm^3) and crystallized by slow diffusion of cyclohexane (50 cm^3). Yield 0.22 g (40%).

X-*Ray Structure Determination*.—Crystal data for compound (**1**) are summarized in Table 2 together with relevant experimental details. Diffraction intensities were collected at room temperature on an Enraf-Nonius CAD-4 diffractometer and reduced to F_o values. An absorption correction was applied by measuring six reflections at $\chi > 80$ (minimum and maximum transmission factors 84—100%). The structure was solved by direct methods and Fourier methods. The SHELX 76[11] package of crystallographic programs was used for all calculations. Thermal vibrations were treated anisotropically for all atoms belonging to the anion, and for the P atoms of the cations. Phenyl rings of the cation were treated as rigid bodies (C–C–C 120°, C–C 1.395 Å) and H atoms were added in calculated positions and refined 'riding' on the corresponding C atoms. A final Fourier map showed residual peaks lower than 1.0 e Å^{-3} in the proximity of the metal atoms. The atomic coordinates are listed in Table 3.

Additional material available from the Cambridge Crystallo-

Table 3. Fractional atomic co-ordinates

Atom	*x*	*y*	*z*	Atom	*x*	*y*	*z*
Co(1)	0.466 09(8)	0.753 78(6)	0.185 54(11)	C(123)	0.650 8(4)	0.582 9(2)	0.871 8(5)
Rh(2)	0.352 10(5)	0.754 90(3)	−0.043 40(6)	C(124)	0.575 3(4)	0.634 6(2)	0.820 4(5)
Rh(3)	0.175 94(5)	0.734 95(3)	0.016 23(6)	C(125)	0.569 4(4)	0.654 1(2)	0.706 0(5)
Rh(4)	0.306 54(5)	0.725 36(3)	0.292 95(6)	C(126)	0.638 9(4)	0.622 0(2)	0.643 0(5)
Rh(6)	0.267 35(6)	0.829 95(3)	0.157 91(7)	C(121)	0.714 4(4)	0.570 3(2)	0.694 4(5)
Co(5)	0.365 63(8)	0.651 53(5)	0.118 82(10)	C(132)	0.638 0(3)	0.500 2(2)	0.433 1(5)
P(1)	0.808 21(15)	0.533 31(9)	0.615 87(18)	C(133)	0.593 9(3)	0.467 7(2)	0.326 7(5)
P(2)	0.159 7(2)	0.085 6(1)	0.446 1(2)	C(134)	0.660 5(3)	0.426 1(2)	0.271 7(5)
C	0.323 1(5)	0.740 3(3)	0.120 6(7)	C(135)	0.771 2(3)	0.417 0(2)	0.323 1(5)
C(1)	0.578 4(9)	0.712 8(7)	0.288 0(16)	C(136)	0.815 2(3)	0.449 4(2)	0.429 5(5)
O(1)	0.652 0(10)	0.690 1(9)	0.368 5(15)	C(131)	0.748 6(3)	0.491 0(2)	0.484 5(5)
C(2)	0.381 1(7)	0.775 5(4)	−0.182 3(10)	C(142)	0.895 1(5)	0.638 9(3)	0.661 2(4)
O(2)	0.401 8(8)	0.788 5(4)	−0.265 1(8)	C(143)	0.936 9(5)	0.686 7(3)	0.631 3(4)
C(3)	0.040 5(8)	0.715 1(4)	−0.040 5(8)	C(144)	0.944 0(5)	0.689 6(3)	0.513 7(4)
O(3)	−0.047 7(6)	0.705 5(4)	−0.070 1(7)	C(145)	0.909 4(5)	0.644 7(3)	0.425 9(4)
C(4)	0.278 2(11)	0.709 6(5)	0.436 5(10)	C(146)	0.867 6(5)	0.596 9(3)	0.455 8(4)
O(4)	0.261 8(10)	0.700 6(4)	0.522 2(9)	C(141)	0.860 5(5)	0.594 0(3)	0.573 4(4)
C(6)	0.246 4(7)	0.915 9(5)	0.160 8(8)	C(212)	0.245 8(4)	−0.012 7(3)	0.597 3(5)
O(6)	0.232 5(7)	0.969 7(4)	0.159 4(8)	C(213)	0.319 2(4)	−0.066 3(3)	0.642 8(5)
C(5)	0.477 4(13)	0.597 9(9)	0.103 5(14)	C(214)	0.405 3(4)	−0.087 5(3)	0.596 1(5)
O(5)	0.554 5(15)	0.567 0(9)	0.097 8(17)	C(215)	0.418 1(4)	−0.055 1(3)	0.504 1(5)
C(7)	0.512 6(8)	0.758 4(5)	0.049 5(9)	C(216)	0.344 7(4)	−0.001 5(3)	0.458 6(5)
O(7)	0.590 1(6)	0.762 6(5)	0.023 1(7)	C(211)	0.258 6(4)	0.019 7(3)	0.505 3(5)
C(8)	0.203 7(7)	0.747 9(4)	−0.145 8(8)	C(222)	0.218 2(3)	0.137 9(3)	0.672 7(5)
O(8)	0.149 5(5)	0.748 6(3)	−0.247 7(6)	C(223)	0.201 9(3)	0.174 0(3)	0.773 1(5)
C(9)	0.116 4(7)	0.827 1(4)	0.056 5(7)	C(224)	0.098 5(3)	0.202 0(3)	0.773 7(5)
O(9)	0.030 3(5)	0.858 5(3)	0.031 8(7)	C(225)	0.011 5(3)	0.193 9(3)	0.673 9(5)
C(10)	0.251 8(6)	0.816 9(4)	0.321 9(9)	C(226)	0.027 8(3)	0.157 9(3)	0.573 4(5)
O(10)	0.220 7(6)	0.851 1(3)	0.395 5(6)	C(221)	0.131 2(3)	0.129 8(3)	0.572 8(5)
C(11)	0.366 3(6)	0.631 1(4)	0.281 7(8)	C(232)	0.277 1(5)	0.170 2(3)	0.422 5(4)
O(11)	0.384 2(6)	0.586 4(3)	0.338 7(6)	C(233)	0.321 9(5)	0.202 9(3)	0.358 5(4)
C(12)	0.471 7(9)	0.832 3(6)	0.244 7(9)	C(234)	0.297 6(5)	0.195 9(3)	0.232 2(4)
O(12)	0.510 1(7)	0.874 1(4)	0.289 7(8)	C(235)	0.228 5(5)	0.156 3(3)	0.169 8(4)
C(13)	0.249 7(13)	0.618 0(6)	0.024 1(11)	C(236)	0.183 6(5)	0.123 7(3)	0.233 7(4)
O(13)	0.203 4(9)	0.581 3(4)	−0.022 7(8)	C(231)	0.207 9(5)	0.130 6(3)	0.360 0(4)
C(112)	0.889 8(3)	0.423 8(2)	0.736 9(5)	C(242)	−0.040 4(4)	0.101 9(2)	0.275 7(5)
C(113)	0.965 3(3)	0.383 1(2)	0.821 0(5)	C(243)	−0.123 4(4)	0.080 9(2)	0.185 8(5)
C(114)	1.063 7(3)	0.399 0(2)	0.884 4(5)	C(244)	−0.120 6(4)	0.017 3(2)	0.163 6(5)
C(115)	1.086 7(3)	0.455 6(2)	0.863 7(5)	C(245)	−0.034 8(4)	−0.025 3(2)	0.231 1(5)
C(116)	1.011 2(3)	0.496 3(2)	0.779 6(5)	C(246)	0.048 3(4)	−0.004 4(2)	0.320 9(5)
C(111)	0.912 7(3)	0.480 4(2)	0.716 2(5)	C(241)	0.045 5(4)	0.059 2(2)	0.343 2(5)
C(122)	0.720 4(4)	0.550 8(2)	0.808 8(5)				

graphic Data Centre comprises H-atom co-ordinates, thermal parameters, and remaining bond lengths and angles.

Acknowledgements

Financial support by Consiglio Nazionale delle Ricerce and Ministero della Publica Instruzione is acknowledged.

References

1 Part 16, V. G. Albano, D. Braga, and S. Martinengo, *J. Chem. Soc., Dalton Trans.*, 1986, 981.
2 V. G. Albano, D. Braga, and S. Martinengo, *J. Chem. Soc., Dalton Trans.*, 1981, 717.
3 B. T. Heaton, L. Strona, and S. Martinengo, *J. Organomet. Chem.*, 1981, **215**, 415.
4 P. Chini, G. Longoni, and V. G. Albano, *Adv. Organomet. Chem.*, 1976, **14**, 285.
5 G. Ciani and S. Martinengo, *J. Organomet. Chem.*, 1986, **306**, C49.
6 D. Braga and B. T. Heaton, *J. Chem. Soc., Chem. Commun.*, 1987, 608.
7 B. F. G. Johnson and R. E. Benfield, *Top. Inorg. Organomet. Stereochem.*, 1981, **12**, 253.
8 D. F. Shriver, 'The Manipulation of Air-Sensitive Compounds,' McGraw-Hill, New York, 1969.
9 L. Garlaschelli, P. Chini, and S. Martinengo, *Gazz. Chim. Ital.*, 1982, **112**, 285.
10 C. L. Nivert, G. H. Williams, and D. Seyferth, *Inorg. Synth.*, 1980, **20**, 234.
11 SHELX 76 system of computer programs, G. M. Sheldrick, Cambridge, 1976.

Received 22*nd June* 1988; *Paper* 8/02488J